SCIENTIFIC REPORTS
natureresearch

OPEN

Gene products and processes contributing to lanthanide homeostasis and methanol metabolism in *Methylorubrum extorquens* AM1

Paula Roszczenko-Jasińska[1,3,9], Huong N. Vu[2,4,9], Gabriel A. Subuyuj[2,5], Ralph Valentine Crisostomo[2,6], James Cai[2], Nicholas F. Lien[2], Erik J. Clippard[2], Elena M. Ayala[2], Richard T. Ngo[2], Fauna Yarza[2,7], Justin P. Wingett[2], Charumathi Raghuraman[2], Caitlin A. Hoeber[2], Norma C. Martinez-Gomez[1,8]✉ & Elizabeth Skovran[2]✉

Lanthanide elements have been recently recognized as "new life metals" yet much remains unknown regarding lanthanide acquisition and homeostasis. In *Methylorubrum extorquens* AM1, the periplasmic lanthanide-dependent methanol dehydrogenase XoxF1 produces formaldehyde, which is lethal if allowed to accumulate. This property enabled a transposon mutagenesis study and growth studies to confirm novel gene products required for XoxF1 function. The identified genes encode an MxaD homolog, an ABC-type transporter, an aminopeptidase, a putative homospermidine synthase, and two genes of unknown function annotated as *orf6* and *orf7*. Lanthanide transport and trafficking genes were also identified. Growth and lanthanide uptake were measured using strains lacking individual lanthanide transport cluster genes, and transmission electron microscopy was used to visualize lanthanide localization. We corroborated previous reports that a TonB-ABC transport system is required for lanthanide incorporation to the cytoplasm. However, cells were able to acclimate over time and bypass the requirement for the TonB outer membrane transporter to allow expression of *xoxF1* and growth. Transcriptional reporter fusions show that excess lanthanides repress the gene encoding the TonB-receptor. Using growth studies along with energy dispersive X-ray spectroscopy and transmission electron microscopy, we demonstrate that lanthanides are stored as cytoplasmic inclusions that resemble polyphosphate granules.

Lanthanide (Ln) metals have long been recognized for their magnetic and superconductive properties and have facilitated the advancement of our communication, green energy, and medical technologies[1–4]. However, it has been less than a decade since an inherent role for Ln in methylotrophic bacteria was described[5–7]. Since these initial reports, bacterial strains that are not considered methylotrophs such as *Pseudomonas putida* and *Bradyrhizobium* sp. have been shown to similarly utilize Ln as cofactors in alcohol dehydrogenase (ADH) enzymes, suggesting the impact of Ln on microbial metabolism may be more widespread than initially thought[8–13].

[1]Department of Microbiology and Molecular Genetics, Michigan State University, East Lansing, USA. [2]Department of Biological Sciences, San José State University, San José, CA, USA. [3]Present address: Institute of Microbiology, University of Warsaw, Warsaw, Poland. [4]Present address: Department of Microbiology, University of Georgia, Athens, GA, USA. [5]Present address: Department of Microbiology and Molecular Genetics, University of California At Davis, Davis, CA, USA. [6]Present address: Molecular Biology Institute, University of California At Los Angeles, Los Angeles, CA, USA. [7]Present address: Department of Biochemistry and Biophysics, University of California At San Francisco, San Francisco, CA, USA. [8]Present address: Department of Plant and Microbial Biology, University of California-Berkeley, Berkeley, California, USA. [9]These authors contributed equally: Paula Roszczenko-Jasińska and Huong N. Vu. ✉email: mart1754@msu.edu; elizabeth.skovran@sjsu.edu

To use methanol as a carbon and energy source, many Gram-negative methylotrophic bacteria first oxidize methanol in the periplasmic space using pyrroloquinoline quinone (PQQ)-dependent ADH enzymes. MxaFI is a two-subunit Ca^{2+}-dependent ADH that was long considered to be the predominant methanol dehydrogenase (MeDH) in nature until Ln-dependent XoxF enzymes were first described in 2011[5]. Since their role in methanol oxidation became apparent, XoxF enzymes have been classified into five phylogenetically distinct clades (Type 1 to 5)[14–16]. In 2016, a Ln-dependent ethanol dehydrogenase was described and named as ExaF based on homology with the Ca^{2+}-dependent Exa ethanol dehydrogenases from *Pseudomonas* and *Rhodopseudomonas* strains, and homology with XoxF- and MxaF-type MeDHs[17,18].

When incorporated into the active site, Ln act as potent Lewis acids to facilitate a hydride transfer from the alcohol to the catalytic PQQ cofactor to prompt alcohol oxidation[19–21]. All methylotrophic PQQ-ADHs are periplasmic enzymes associated with a cytochrome c_L (MxaG, XoxG, and ExaG, respectively) that transfers electrons from PQQ to additional cytochromes in the electron transport chain. In addition to the partnering cytochrome c_L, operons or genomic clusters that encode *xoxF* and *exaF* genes often contain homologs of *mxaJ* (*xoxJ* and *exaJ* genes respectively), which encode periplasmic binding proteins that have been suggested to function in the activation of the ADHs [22]. *mxa* operons encode additional proteins that are suggested to function in Ca^{2+} insertion, facilitate interactions between MxaFI MeDH and its cytochrome, and are required for regulation of the *mxa* operon expression[23].

Methylorubrum extorquens AM1 (formerly *Methylobacterium extorquens* AM1) produces a MxaFI-type MeDH (encoded by *mxaF: MexAM1_META1p4538* and *mxaI: MexAM1_META1p4535*), two XoxF (type 5) MeDHs (encoded by *xoxF1*: *MexAM1_META1p1740* and *xoxF2*: *MexAM1_META1p2757*), and an ExaF-type ethanol dehydrogenase (encoded by *exaF*: *MexAM1_META1p1139*)[17,18]. The XoxF enzymes from *M. extorquens* AM1 share 90% amino acid similarity, and are named as XoxF1 and XoxF2 to distinguish them from one another[24]. Phenotypic studies suggest *M. extorquens* AM1 XoxF1 and XoxF2 have redundant function[18]. However, in the laboratory, XoxF1 appears to be the dominant XoxF-MeDH as *xoxF2* is expressed at low levels[18,25]. A fifth putative PQQ-ADH encoded by *MexAM1_META1p4973* does not contribute to methanol growth under the conditions tested[17]. When Ln are absent, MxaFI is the only known contributor to methanol oxidation in *M. extorquens* AM1. When Ln are available, the XoxF enzymes produce formaldehyde from methanol whereas ExaF oxidizes methanol further to formate[25].

In addition to catalysis, Ln serve as a signal for a transcriptional response called "the Ln-switch" or "rare earth-switch," though the mechanism of Ln signal sensing is not completely understood[18,26–29]. When Ln are available, the *mxa* operon (*mxaFJGIRSACKLDEHB*) is downregulated and transcript levels of the *xox1* operon genes (*xoxF$_1$GJ*) are upregulated[18,25–28]. In *M. extorquens* AM1 and closely related PA1 strain, the MxbDM two-component system along with the *xoxF1* and *xoxF2* genes themselves have been shown to be required for operation of the Ln-switch[24,30,31]. However, suppressor mutations in the *mxbD* sensor kinase encoding gene can arise, which bypass the need for XoxF1 and XoxF2, presumably by constitutively activating the MxbM response regulator[24,29,31]. Though much progress has been made regarding the catalytic and regulatory roles of Ln in methylotrophic bacteria, relatively little is known about how these Ln are acquired and incorporated into the enzymes that use them.

The machinery necessary for Ln transport is in the early stages of characterization and is predicted to be analogous to siderophore-mediated iron transport[4,31] with the siderophore-like molecule referred to as a lanthanophore[32]. In *M. extorquens* AM1, ten genes predicted to encode proteins involved in Ln transport and utilization are clustered together in the genome (*MexAM1_META1p1778*–*MexAM1_META1p1787*) and encode an ABC-type transporter, four hypothetical periplasmic proteins of unknown function, a periplasmic protein that binds Ln (encoded by *MexAM1_META1p1781*), a TonB-dependent transporter, and lanmodulin (encoded by *MexAM1_META1p1786*)[4,33]. In closely related *M. extorquens* strain PA1, Ochsner et al. characterized the Ln transport cluster by generating deletions spanning multiple genes in the predicted transport system[31]. Their results showed that a TonB-dependent transporter and a putative ABC transporter were necessary for Ln transport, suggesting Ln transport into the cytosol. A detailed analysis of the contribution of each gene from the transport cluster is still lacking and Ln transport has not been quantified. Subsequently, Mattocks et al. demonstrated that in strain AM1 the hypothetical periplasmic protein encoded by *MexAM1_META1p1781* efficiently binds lighter Ln and that similar to strain PA1, Ln are transported into the cytosol[4].

In this study, we describe new pieces necessary to complete the Ln puzzle: the identification of novel genes that contribute to Ln metabolism and methanol oxidation, and the discovery and visualization of Ln storage in *M. extorquens* AM1. Detailed growth studies for strains lacking each component of the first eight genes in the Ln transport cluster are described, including the ability of these strains to mutate or acclimate (phenotypic change that is inducible and reversible) to allow Ln transport through a predicted secondary mechanism. Ln uptake is also quantified for several transport mutant strains. Finally, we show that *M. extorquens* AM1 stores Ln with phosphate as crystalline cytoplasmic deposits.

Results

A genetic study identifies gene products that contribute to methanol oxidation.

A transposon mutagenesis study was designed to take advantage of the in vivo formaldehyde production capability of XoxF1 and XoxF2 to identify genes required for XoxF-dependent methanol oxidation. The strain used to conduct the mutant hunt contained a mutation in *mxaF* to make cells dependent on the exogenously provided La^{3+} for formaldehyde production, and a second mutation in *fae*, which would result in formaldehyde accumulation and cell death when methanol is oxidized to formaldehyde by XoxF1 and XoxF2 (Fig. 1). Transposon insertions that reduced or eliminated formaldehyde production allowed survival and colony formation on media containing both methanol and succinate, since methanol resistant strains could use succinate for growth. In addition to

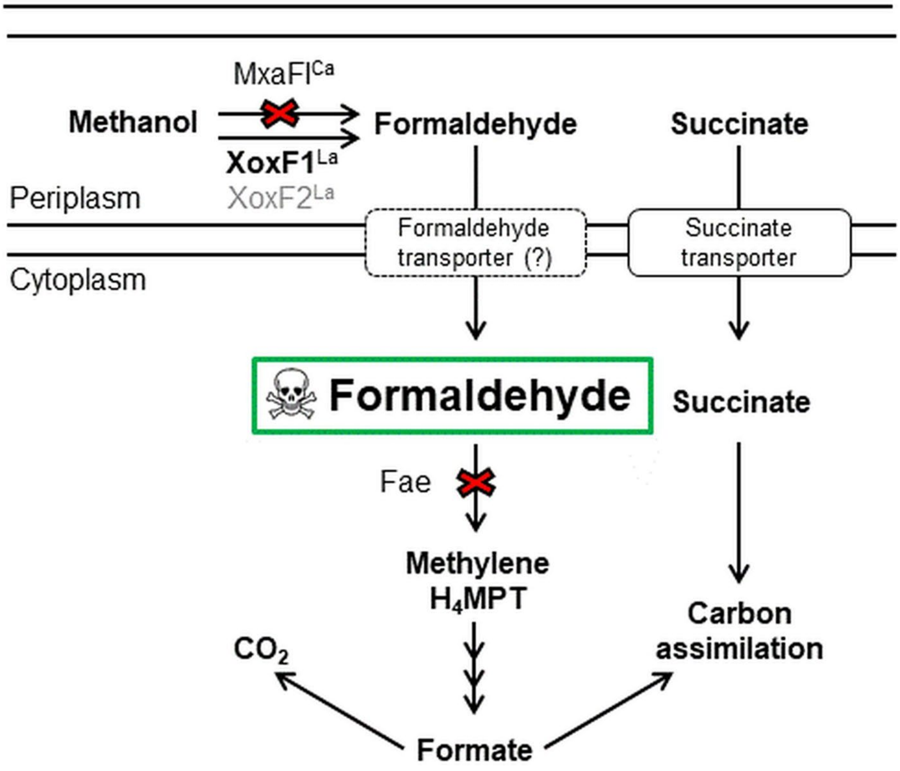

Figure 1. Schematic representation of the metabolic processes relevant to the *mxaF fae* transposon mutagenesis study. XoxF1 and XoxF2 oxidize methanol to formaldehyde, which accumulates to lethal levels in the *fae* mutant strain. If a process required for XoxF-dependent methanol oxidation is disrupted by a transposon insertion, formaldehyde is reduced or eliminated, and cells use succinate for growth. A dashed line around the formaldehyde transporter is to indicate that this function has not been demonstrated.

genes required for XoxF1 and XoxF2 function, this mutant hunt had the potential to identify a hypothetical formaldehyde import system, disruption of which might reduce formaldehyde levels in the cytoplasm (Fig. 1). As ExaF oxidizes methanol directly to formate[25], *exaF* and genes specific to ExaF function were not expected to be identified though this genetic study.

Over six hundred transposon mutants were isolated, and their insertion locations mapped to the *M. extorquens* AM1 genome. As it is likely that a portion of these transposon mutants became methanol-resistant due to spontaneous second-site suppressor mutations and not the transposon insertion, only genes that were independently identified four or more times were considered for further analysis and are listed in Table 1. From the twenty eight genes identified in our transposon mutagenesis study (Table 1), mutations in twenty three genes were constructed in *mxaF* and/or wild-type strain backgrounds and methanol growth in the presence of La^{3+} was assessed (Tables 2, 3).

Growth phenotypes of strains lacking genes identified in the transposon mutagenesis study. Novel genes were identified in the transposon mutagenesis study which impacted methanol growth with La^{3+} when deleted from the *M. extorquens* AM1 genome (Table 1). The identified genes encode a LysR-type transcriptional regulator (*MexAM1_META1p0863*), two proteins of unknown function annotated as *orf6* and *orf7* (*MexAM1_META1p1746* and *MexAM1_META1p1747* respectively), an MxaD homolog (*MexAM1_META1p1771*), a putative homospermidine synthase (*MexAM1_META1p2024*), an ABC-type transporter (*MexAM1_META1p2359*), and an aminopeptidase (*MexAM1_META1p3908*). Growth rates for strains lacking these genes are shown in Table 2 and growth curves for mutant strains that had a 30% or greater reduction in growth rate are shown in Fig. 2a–f. Among these identified genes, loss of the *MexAM1_META1p2359* ABC-type transporter, putative homospermidine synthase, and lysR-type regulator resulted in similar growth defects in the absence of La^{3+} (Table S1) which suggests an involvement in both XoxF1- and MxaFI-facilitated methanol growth. The identification of these genes and initial growth studies lay the foundation to explore the specific roles and requirements for these gene products in methanol oxidation.

Also included in the list of genes identified in the transposon mutagenesis study were those that encode proteins with described roles in methanol oxidation (PQQ biosynthesis, *xoxF1, xoxG, xoxJ*) and those with predicted functions based on sequence similarity (cytochrome synthesis and Ln transport[31,34]). Deletion of PQQ biosynthesis genes (Δ*pqqBCDE*; Δ*pqqF*) and genes in the three identified cytochrome *c* biogenesis and heme export clusters[34] (*cycK*; *ccmB*; *ccmC*) eliminated methanol growth in the presence and absence of La^{3+} as expected (Tables 2, S1).

Gene designation	Gene name	Predicted function
MexAM1_META1p0863		LysR-type regulator
MexAM1_META1p1292	*cycL*	*c*-type cytochrome biogenesis
MexAM1_META1p1293	*cycK*	Heme lyase
MexAM1_META1p1294	*cycJ*	Periplasmic heme chaperone
MexAM1_META1p1740	*xoxF1*	Ln-dependent methanol dehydrogenase
MexAM1_META1p1741	*xoxG*	Cytochrome *c*
MexAM1_META1p1742	*xoxJ*	Periplasmic binding protein
MexAM1_META1p1746	*orf6*	Unknown
MexAM1_META1p1747	*orf7*	Unknown
MexAM1_META1p1748	*pqqE*	PQQ biosynthesis
MexAM1_META1p1749	*pqqCD*	PQQ biosynthesis
MexAM1_META1p1750	*pqqB*	PQQ biosynthesis
MexAM1_META1p1771		MxaD homolog
MexAM1_META1p1778	*lutA*	ABC transporter-periplasmic binding component
MexAM1_META1p1779	*lutB*	Exported protein
MexAM1_META1p1782	*lutE*	ABC transporter-ATP binding component
MexAM1_META1p1783	*lutF*	ABC transporter-membrane component
MexAM1_META1p1784	*lutG*	Exported protein
MexAM1_META1p1785	*lutH*	TonB-dependent receptor
MexAM1_META1p2024	*hss*	Homospermidine synthase
MexAM1_META1p2330	*pqqF*	Protease
MexAM1_META1p2331	*pqqG*	Protease
MexAM1_META1p2359		ABC transporter—fused ATPase and transmembrane components
MexAM1_META1p2732	*ccmC*	Heme export
MexAM1_META1p2734	*ccmG*	*c*-type cytochrome biogenesis
MexAM1_META1p2825	*ccmB*	Heme export
MexAM1_META1p2826	*ccmA*	Heme export
MexAM1_META1p3908		Leucyl aminopeptidase

Table 1. Genes identified four or more times via transposon mutagenesis.

XoxF1 and XoxF2 catalytically contribute to methanol oxidation and growth when methanol and Ln are provided [17,18], and exert a regulatory role in the absence of Ln as production of XoxF1 or XoxF2 is required for expression of the Ca^{2+}-dependent MxaFI-MeDH[18,24]. Growth analysis and transcriptional reporter fusion studies were employed to see if strains lacking *xoxG* or *xoxJ* had similar effects on growth and *mxa* operon expression. In methanol La^{3+} medium, loss of either *xoxG* or *xoxJ* was equivalent to loss of both *xoxF1* and *xoxF2* (Fig. 3; Table 3), which is consistent with XoxG and XoxJ being essential for XoxF-dependent methanol oxidation as suggested by recent biochemical studies[22,35,36].

Unlike the *xoxF1 xoxF2* double mutant strain, transcriptional reporter fusion studies that assessed expression from the *mxa* promoter determined that the growth phenotypes observed for the *xoxG* and *xoxJ* mutants grown in the absence of La^{3+} were not due to impaired *mxa* expression (Table 4). Taken together, these phenotypes suggest XoxG and XoxJ may play a broader role in methanol metabolism in *M. extorquens* AM1 independent from facilitating XoxF1 and XoxF2 catalytic and regulatory functions.

Detailed phenotypic characterization of Ln utilization and transport cluster mutant strains..

Consistent with previous reports for strain PA1, our transposon mutagenesis studies suggest that genes encoding homologs of the TonB- and ABC-dependent Fe^{3+} scavenging systems play a role in methanol metabolism when Ln are present[31]. In addition to the transport system homologs, two of six hypothetical periplasmic proteins encoded in the Ln transport cluster were identified in the transposon mutagenesis study (Fig. 4a). We expanded Ochsner's study by dissecting the contribution of individual genes (*MexAM1_META1p1778* through *MexAM1_META1p1785*). Based upon work detailed within, we propose to name the Ln transport cluster genes as *lut*, for Ln utilization and transport.

As reported by Ochsner et al.[31], loss of *lutH* (*Mextp1853* in strain PA1) alone did not result in a growth defect in medium containing methanol and La^{3+}, which is consistent with the hypothesis that the TonB-dependent transporter is needed for transport of La^{3+} into the periplasm. If La^{3+} does not enter the periplasm, the *mxaF* and *mxaI* genes are likely expressed and used for methanol oxidation. Loss of both *mxaF* and *lutH* arrested growth, but after 90–120 h, growth of the *mxaF lutH* double mutant strain occurred in approximately 60% of the 24 cultures tested (Fig. 4c; Tables 2, 5). Consistent with an acclimation process and not a suppressor mutation, the *mxaF lutH* double mutant strain lost the ability to grow in methanol medium with La^{3+} after passage onto medium containing succinate. To determine if acclimated growth was due to production of XoxF1, expression from the *mxa* and *xox1* promoters was measured before and after acclimation (Table 4). Before acclimation, *mxa*

Strain	Growth rate (h^{-1})[a] in MeOH + La^{3+}
Growth of control strains	
Wild type	0.16 ± 0.01
mxaF	0.16 ± 0.01
xoxF1	6–9 h lag, 0.07 ± 0.00
xoxF1 xoxF2	6 h lag, 0.04 ± 0.01
mxaF xoxF1 xoxF2	6 h lag, 0.04 ± 0.00
Growth of strains lacking novel genes identified in genetic selection	
MexAM1_META1p0863	0.14 ± 0.00
MexAM1_META1p1771	0.11 ± 0.01
orf6	0.03 ± 0.00
orf7	9 h lag, 0.08 ± 0.01
MexAM1_META1p2359	No growth
hss	6 h lag, 0.10 ± 0.01
MexAM1_META1p3908	15 h lag, 0.07 ± 0.00
Growth of strains lacking genes with known function	
pqqBCDE	No growth
pqqF	No growth
cycK	No growth
ccmB	No growth
ccmC	No growth
Growth of strains lacking lanthanide utilization and transport genes	
lutA	0.02 ± 0.01, 96 h; 0.08 ± 0.01
mxaF lutA	0.02 ± 0.00
lutB	0.02 ± 0.00, 87 h; 0.05 ± 0.01
mxaF lutB	0.02 ± 0.00
lutC	9 h lag, 0.11 ± 0.01
mxaF lutC	9 h lag, 0.11 ± 0.01
lutE	No growth
mxaF lutE	No growth
lutF	No growth
mxaF lutF	No growth
lutG	12 h lag, 0.03 ± 0.00
mxaF lutG	12 h lag, 0.03 ± 0.00
lutH	0.16 ± 0.00
mxaF lutH	No growth

Table 2. Growth parameters for strains grown in methanol medium with La^{3+}. [a]Data for a minimum of three biological replicates are reported. ±Indicates standard deviations.

Strain	Growth rate (h^{-1})[a]	
	MeOH	MeOH + La^{3+}
Wild type	0.14 ± 0.01	0.16 ± 0.01
xoxF1 xoxF2	No growth	6 h lag, 0.04 ± 0.01
xoxG	3 h lag, 0.11 ± 0.01	0.04 ± 0.00
xoxJ	21 h lag, 0.13 ± 0.00	0.04 ± 0.01

Table 3. Growth parameters for *xox* strains grown in methanol medium with and without La^{3+}. [a]Data for a minimum of three biological replicates are reported. ±Indicates standard deviations.

promoter expression occurred at levels comparable to those in media lacking La^{3+} in the wild-type strain while *xox1* expression was repressed as the cells could not transport La^{3+} to promote the Ln-switch. Once acclimation occurred and the *mxaF lutH* strain began to grow, expression from the *mxa* promoter was repressed and expression from the *xox1* promoter was induced, suggesting the cells were able to uptake La^{3+} through the outer membrane via an unknown mechanism.

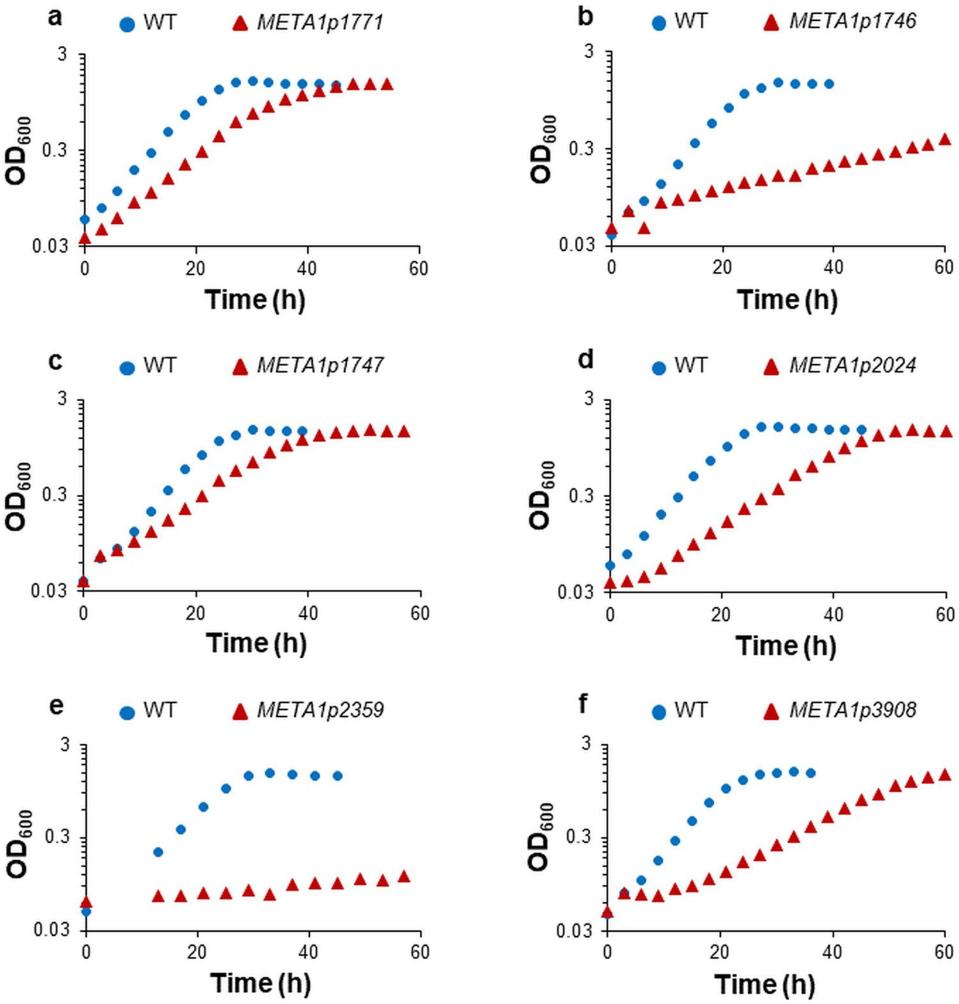

Figure 2. Growth of mutant strains lacking genes identified through transposon mutagenesis in medium containing methanol and La^{3+}. Growth of *M. extorquens* AM1 wild-type is represented by blue circles and depicted mutant strains (red triangles) have the following genes deleted: (**a**) *MexAM1_META1p1771*, *mxaD* homolog; (**b**) *MexAM1_META1p1746*, *orf6*; (**c**) *MexAM1_META1p1747*, *orf7*; (**d**) *MexAM1_META1p2024*, homospermidine synthase; (**e**) *MexAM1_META1p2359*, ABC transporter of unknown function; (**f**) *MexAM1_META1p3908*, aminopeptidase. Representative data from biological triplicates are shown. One-way analysis of variance (ANOVA) determined that growth rate differences between mutant and parent strains are significantly different ($p < 0.005$).

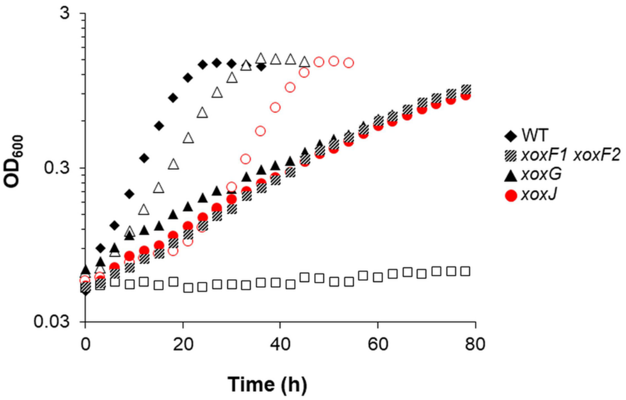

Figure 3. Growth of *xoxG* and *xoxJ* mutant strains in the presence (filled symbols) and absence (open symbols) of La^{3+}. Representative data from biological triplicates are shown. One-way analysis of variance (ANOVA) determined that growth rate differences between mutant and parent strains are significantly different ($p < 0.005$).

	MeOH		MeOH + La^{3+}	
Promoter	***mxa***	***xox1***	***mxa***	***xox1***
Strain				
Wild type	323 ± 63	44 ± 3	61 ± 10	206 ± 11
mxaF lutH	ND	ND	363 ± 11	53 ± 7
mxaF lutH acclimated	ND	ND	82 ± 14	240 ± 17
xoxF1 xoxF2	25 ± 4	ND	ND	ND
xoxG	365 ± 24	ND	ND	ND
xoxJ	566 ± 55	ND	ND	ND

Table 4. Expression from *mxa* and *xox1* promoters (RFU/OD$_{600}$) in wild type and mutant strains grown in methanol media with or without La^{3+} (Data for a minimum of three biological replicates is reported). *ND* not determined.

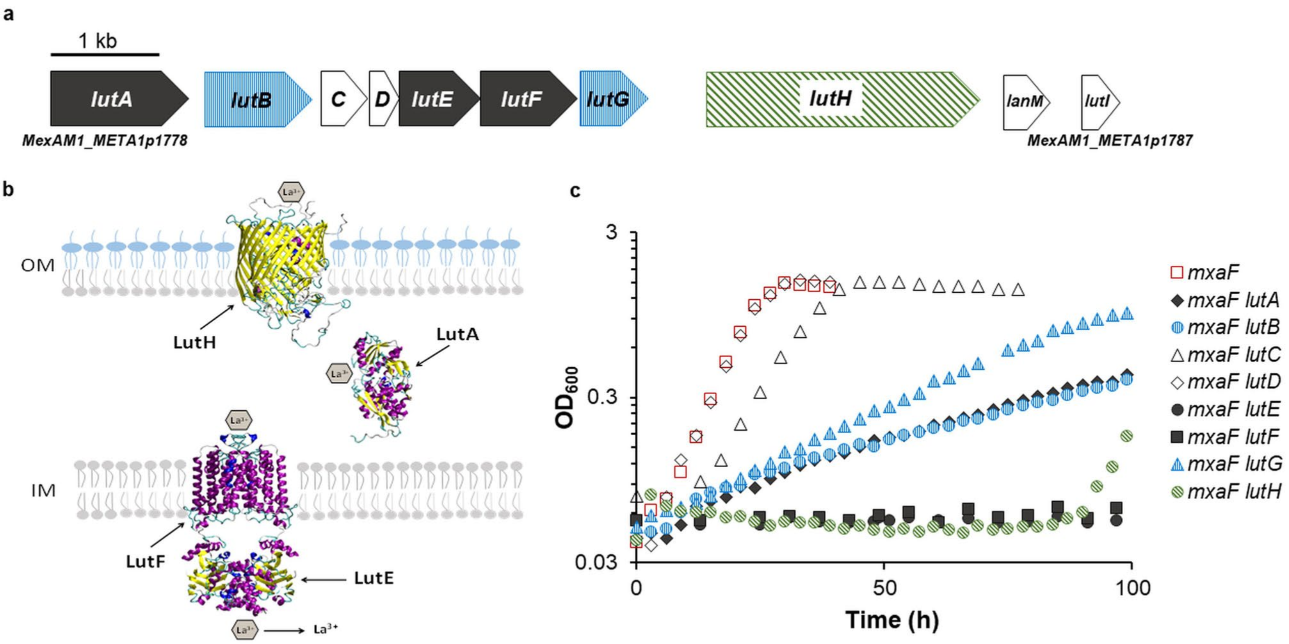

Figure 4. Characterization of the *lut* cluster. (**a**) Genomic map of the *lut* genes (*MexAM1_META1p1778* to *MexAM1_META1p1787*). Black, genes encoding the ABC transport system; green, gene encoding the TonB-dependent transporter; blue, genes encoding putative periplasmic proteins identified by transposon mutagenesis; white, lanmodulin and additional genes encoding periplasmic proteins not identified by transposon mutagenesis. (**b**) Model for Ln transport. The three-dimensional structures of monomers of LutH and LutA were predicted using homology modeling (HHpredserver and MODELLER)[37] and homodimers of the ABC transporter were predicted using GalaxyHomomer[38]. (**c**) Growth of *mxaF* and *mxaF lut* mutant strains with 2 µM LaCl$_3$. Graphs depict representative data from three biological replicates. Growth rate averages and standard deviations are shown in Table 2.

	MeOH + La^{3+}	
	Time of S/A	**Growth rate**^{a}
Strain	**(h)**	**(h^{-1})**
MexAM1_META1p2359	Suppressor: 85	0.10 ± 0.01
lutE	Suppressor: 75–90	0.07 ± 0.01
mxaF lutE	Suppressor: 200–220	0.02 ± 0.00
lutF	Suppressor: 79–91	0.09 ± 0.02
mxaF lutF	Suppressor: 145–157	0.02 ± 0.01
mxaF lutH	Acclimation: 90–120	0.14 ± 0.02

Table 5. Growth parameters of suppressor and acclimation events. ^{a}Data for a minimum of three biological replicates is reported.

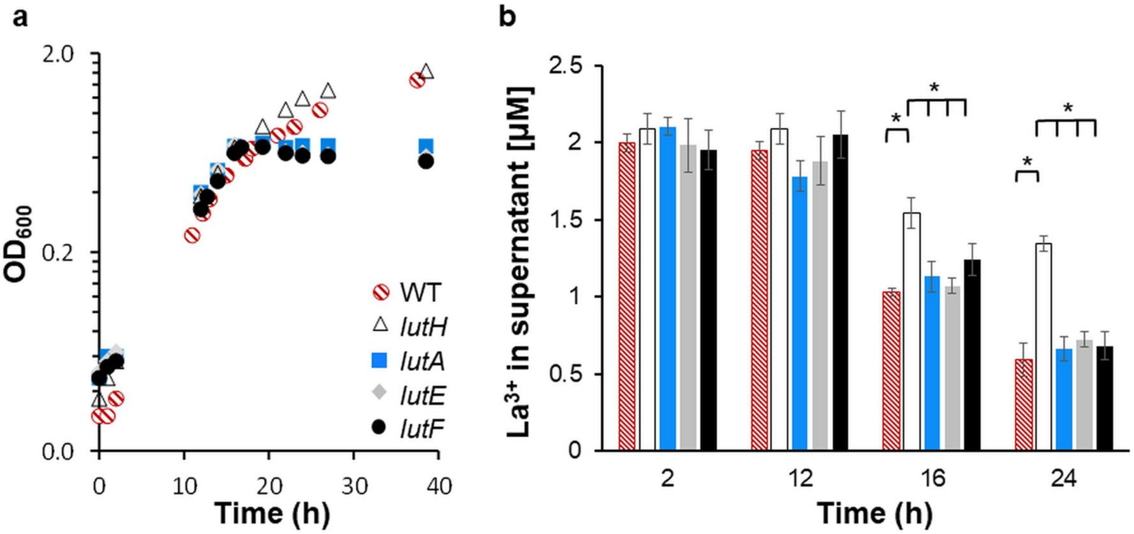

Figure 5. Growth studies and measurement of La^{3+} uptake suggest La^{3+} storage capability. (**a**) Growth of wild type (red dashed circles), *lutH* (white triangles), *lutA* (blue squares), *lutE* (gray diamonds), and *lutF* (black circles) strains grown with limiting succinate (3.75 mM), methanol (125 mM), and 2 μM LaCl$_3$. Data are the average of three biological replicates. Standard deviations between biological replicates were less than ± 0.02. (**b**) La^{3+} concentrations (μM) in culture supernatants of *lut* mutant strains depicted in same color code as in (**a**). Data depict the average of three biological replicates with error bars showing the standard deviation. One-way analysis of variance (ANOVA) followed by a t-test was used to represent statistical significance. *The *p*-value is < 0.005.

LutA, a periplasmic binding protein, is predicted to traffic lanthanophore bound Ln through the periplasm to the inner membrane transporter system (encoded by *lutE* and *lutF*) for transport into the cytoplasm (Fig. 4b). Strains lacking *lutE* or *lutF* in the *mxaF* mutant strain background were unable to grow in medium containing methanol and La^{3+} (Fig. 4c, Table 2). However, after 200 h and 150 h respectively, second-site suppressor mutations arose which facilitated growth albeit 88% slower than that of the wild-type strain (Table 5). In contrast, loss of *lutA* in the absence of *mxaF* still allowed La^{3+}-dependent growth but at a reduced rate (Fig. 4c). Genes *lutB* and *lutG*, encoding hypothetical periplasmic proteins, were also identified in the transposon mutagenesis study. Growth of the *mxaF lutB* and *mxaF lutG* double mutant strains was similar to that of the *mxaF lutA* double mutant strain, suggesting an equally important but non-essential function. The growth observed for the *lutA*, *lutB*, and *lutG* mutant strains in the absence of *mxaF* was not identified as acclimation or second-site suppression. To ensure that observed phenotypes were not due to polarity, mutants lacking individual transport cluster genes (*lutABEFG*) were complemented by expressing the respective gene in pCM62[39] and growth similar to the wild-type strain was restored in each case (Fig. S1).

Genes encoding LutC, LutD, LanM, and LutI were not identified in the transposon study but LutD and LanM have been shown to bind Ln[4,33]. Loss of *lutD* did not result in a significant growth defect in the *mxaF* mutant and wild-type strain backgrounds while loss of *lutC* resulted in a small growth defect when La^{3+} was provided (Fig. 4c; Table 2).

Quantification of La^{3+} uptake. To assess how loss of the Ln transport system affects La^{3+} uptake, La^{3+} levels were quantified from the spent media at different phases of growth (Fig. 5). Strains were grown in methanol medium containing 2 μM LaCl$_3$ and limiting succinate (3.75 mM) as *lutA, lutE,* and *lutF* mutant strains are unable to grow or grow poorly with methanol as a sole carbon source (Fig. 4c; Table 2). While significant decreases in La^{3+} levels were not observed for any strain during early- to mid-exponential phase (Fig. 5a,b), as cultures continued to grow, and succinate was likely depleted, significant differences in La^{3+} levels became apparent. In the wild-type strain, La^{3+} uptake continued into stationary phase (Fig. 5a,b). Growth of the *lutE* and *lutF* mutants (encoding ABC-transporter components) was arrested at an approximate OD$_{600}$ of 0.7 (Fig. 5a), yet La^{3+} concentrations in the spent media continued to decrease to 0.7 μM eight hours into stationary phase (Fig. 5b). Taken together with the growth phenotypes, these data suggest that in the absence of the Lut-ABC-transporter system, Ln are likely transported through the outer membrane into the periplasm but cannot enter the cytoplasm. Levels of La^{3+} in the supernatants from the *lutH* TonB-dependent transporter mutant were significantly higher than wild type in mid-exponential and stationary phases (Fig. 5b). However, a small decrease in La^{3+} content from the *lutH* mutant strain culture supernatants was observed.

Expression from the *lutH* promoter is repressed by La^{3+}. Genes found within the *lut* cluster are likely not expressed as a single transcript as suggested by the spacing between genes such as *lutG* and *lutH*, and by multiple promoters predicted by the bacterial promoter prediction tool, BPROM[40]. To test if expression of the of Ln uptake genes is regulated by Ln, a fluorescent transcriptional reporter fusion was used to monitor expression

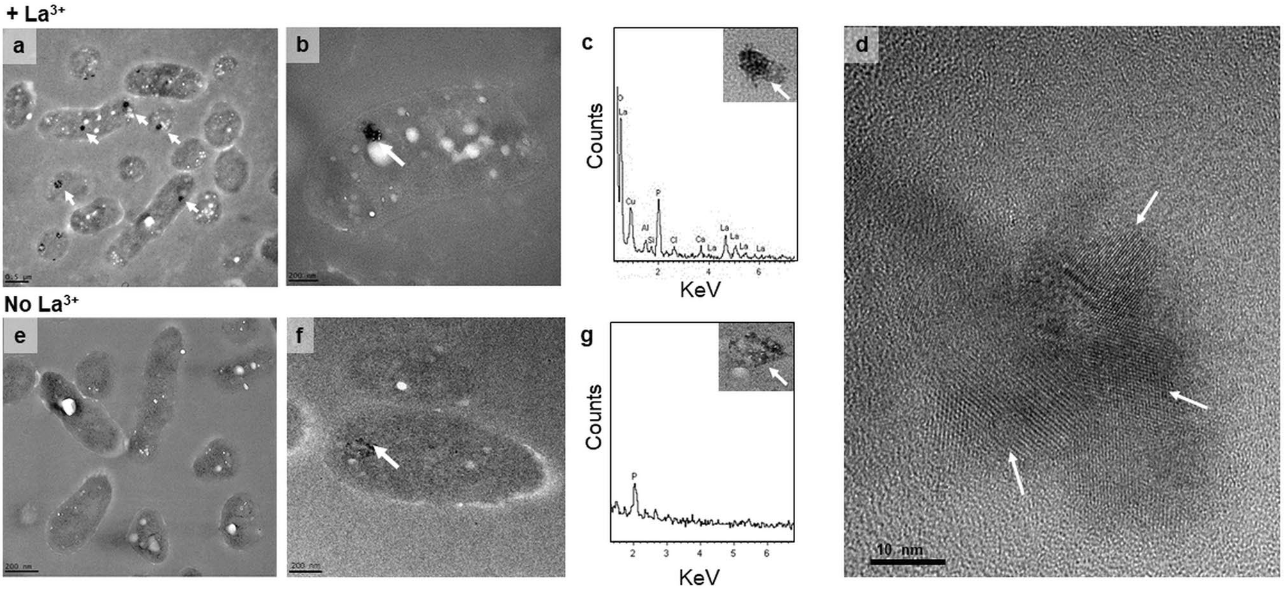

Figure 6. Visualization of La^{3+} storage. TEM of ultrathin sections of wild-type cells harvested at OD_{600} of ~ 0.6 after growth with 3.75 mM succinate and 125 mM methanol containing (**a**, **b**) and lacking (**e**, **f**) 20 µM La^{3+}. (**c**, **g**) Elemental analysis of electron dense deposits from cells grown with (**c**) and without (**g**) La^{3+}. (**d**) High-resolution transmission electron microscopy analysis of the wild-type strain shows an atomic lattice structure in electron-dense areas suggesting that La^{3+} is embedded in cytoplasmic crystals.

from the predicted *lutH* promoter region in methanol media. Addition of exogenous La^{3+} repressed expression fourfold (RFU/OD_{600}: 210 ± 7 without La^{3+} and 47 ± 5 with La^{3+}) showing that when Ln are in excess, transport is down-regulated. Similar repression has been reported for transcription of the TonB-dependent transporter of *Methylotuvimicrobium buryatense* 5GB1C[41].

La^{3+} is stored as cytoplasmic crystalline deposits. Transmission electron microscopy (TEM) coupled with energy dispersive X-ray spectroscopy (EDS) has been used to determine the elemental composition of cellular inclusions[40,42] while La^{3+} has been widely used as an intracellular and periplasmic stain for electron microscopy[43–45]. Here, we show that La^{3+} can be directly identified by TEM if accumulated inside *M. extorquens* AM1 cells. Electron-dense deposits were observed in the cytoplasm from *M. extorquens* AM1 cells grown with exogenous $LaCl_3$ (Fig. 6a,b). Samples were analyzed using EDS and corroborated that the electron dense deposits contained La^{3+} (Fig. 6c). When grown without La^{3+}, only a few cells showed smaller electron dense areas (Fig. 6e, f); however, La^{3+} was not detected in EDS analysis in these cases (Fig. 6g). These data demonstrate that La^{3+} can be stored in *M. extorquens* as metal deposits. Moreover, EDS analysis of electron dense areas from the wild-type strain grown with La^{3+} determined a content of lanthanum (22.2 ± 1.0 weight %), phosphorus (15.1 ± 2.1 weight %), and oxygen (51.1 ± 1.9 weight %), suggesting La^{3+} is complexed with phosphates (Fig. S2). Traces of chloride (3.0 ± 1.0 weight %), calcium (2.2 ± 0.6 weight %), and aluminum (3.4 ± 0.6 weight %) ions were also detected. The copper, carbon, and silicon ion content from the support grids and embedding medium were not considered for metal content calculations. High-resolution transmission electron microscopy (HRTEM) images of the La^{3+} deposits showed an atomic lattice with a Moiré fringes pattern, indicating a crystalline nature[46] (Fig. 6d). Together, these results suggest that La^{3+} is embedded in inorganic phosphate crystals, which form the electron dense deposits observed in the cytoplasm.

Visualization of La^{3+} accumulation in *lut* transporter mutants. To determine if La^{3+} could be visualized in strains lacking the Lut-TonB-ABC transport system, TEM and EDS were employed for the analysis of *lutA*, *lutE*, *lutF*, and *lutH* mutant strains. Strains were grown in methanol medium containing La^{3+} and limiting succinate. Samples stained with OsO_4 and 2% uranyl acetate allowed the outer and inner membrane of the bacterial cells to be distinguished (Fig. 7a–e and g left subpanels), while visualization without staining enabled metal content analysis by removing the interaction between Os^{8+} and phosphate, which interferes with La^{3+} measurements (Fig. 7a–e and g right subpanels). Mutants lacking the TonB-dependent transporter (encoded by *lutH*) did not display La^{3+} deposits (Fig. 7a compared to Fig. 7g). In contrast, localized La^{3+} deposits were visualized in the periplasmic space in mutant strains lacking the ABC-transporter components (encoded by *lutA, lutE*, and *lutF*) as shown in Fig. 7b–e. EDS microanalyses confirmed these electron dense periplasmic deposition areas contained La^{3+} (Fig. 7f). Taken together, these findings directly demonstrate a role for the TonB-dependent and ABC transporters in Ln transport.

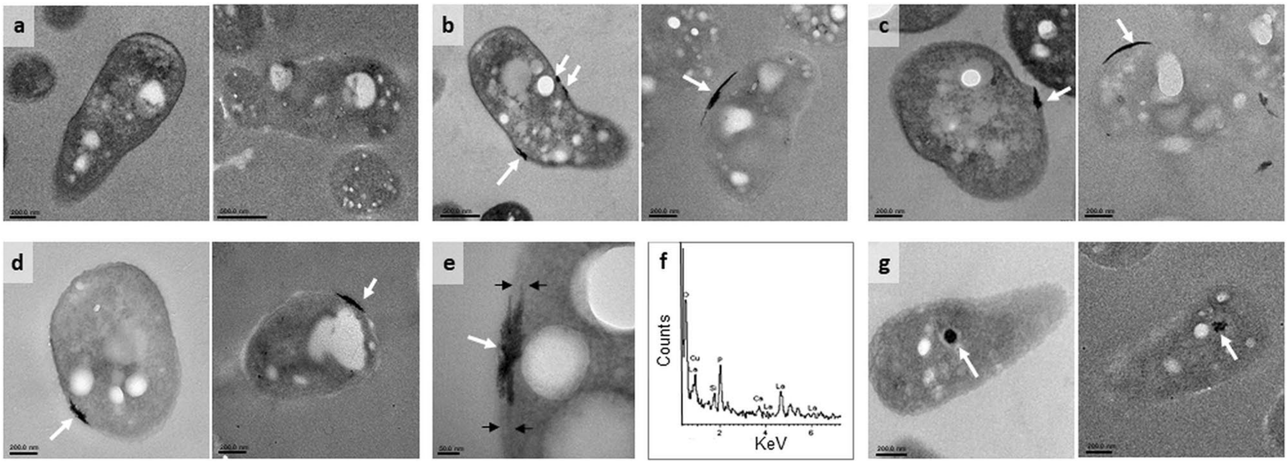

Figure 7 . Visualization of La^{3+} localization using TEM. Thin sections of (**a**) *lutH*, (**b**) *lutE*, (**c**) *lutF*, (**d**) *lutA*, and (**g**) wild-type strains grown with 3.75 mM succinate, 125 mM methanol, and 20 µM $LaCl_3$. White arrows indicate deposits of electron scattering material in the periplasm. Cells were fixed with 2.5% glutaraldehyde and stained with OsO_4 and uranyl acetate to detect cell membranes (left subpanel) or left unstained for elemental analysis (right subpanel). (**e**) Magnification of the La^{3+}-deposits localized in the periplasmic space from the *lutA* mutant strain; black arrows indicate the boundaries of the outer membrane and inner membrane of the *lutA* mutant strain. (**f**) Elemental analysis of the electron-dense deposits observed inside the periplasm.

Discussion

The Ln-dependent XoxF1-MeDH produces formaldehyde in vivo[25]. Here, we took advantage of this property which allowed lethal levels of formaldehyde to accumulate when methanol was oxidized by XoxF1 and *fae* was deleted from the genome. These phenotypes enabled a genetic selection to identify gene products required for or involved in XoxF1-mediated methanol oxidation.

Ln must be transported into the cell and incorporated into the XoxF1 active site[25,47] but is not yet known if incorporation occurs in the cytoplasm or periplasmic space. Our growth, transport, TEM, and EDS analyses are consistent with LutH facilitating Ln transport into the periplasm and the Ln-ABC transport system facilitating Ln transport into the cytoplasm. La^{3+} concentrations found in the supernatant from strain variants lacking transport system components suggest that once in the periplasm, significant concentrations of La^{3+} do not go back outside of the cell as ABC transporter mutant strains showed uptake of La^{3+} from the medium similar to the wild-type strain. Intriguingly, TEM and EDS studies with ABC transporter mutant strains demonstrated localized accumulation of La^{3+} in the periplasmic space. It is not yet clear how or why La^{3+} accumulates in specific areas rather than appears diffused throughout the periplasm.

In *M. extorquens*, the MxbDM two-component system has been proposed to sense periplasmic Ln either directly or indirectly to facilitate differential regulation of the *mxa* and *xox1* operons[18,31]. Results from our growth, transport, and visualization studies support the hypothesis by Oschner et al.[31] that the regulatory network controlling differential expression may be more complex than initially thought. Consistent with Ochsner et al. and Mattocks et al., our data suggest Ln must enter the cytoplasm for *xoxF1* to be expressed[4,31]; *lut* ABC transporter mutants accumulated La^{3+} in the periplasmic space yet were unable to grow. It is also possible that *xoxF1* is expressed and produced in the *lut* ABC transporter mutants, yet periplasmic La^{3+} is not incorporated into the active site of XoxF1 as it is bound by lanthanophores. It is not yet known if Ln release from the lanthanophore occurs in the periplasm, or if Ln are first released in the cytoplasm then exported back into the periplasmic space for insertion into XoxF1. While a LysR-type transcriptional regulator was identified multiple times in this genetic study, no severe growth defect was observed when disrupted.

Our data also suggest periplasmic Ln may be enough to prevent *mxa* expression since the *lut* ABC transporter mutants could not grow when *mxaF* was intact in the genome. An analogous system in *P. putida* KT2440 exists where expression of the *pedH* and *pedE* genes, which encode Ln- and Ca-dependent ADHs respectively, are differentially regulated by Ln through the PedS2/R2 two-component system[10]. Unlike *M. extorquens*, Ln-ABC transport mutants of *P. putida* KT2440 express *pedH* when Ln are present, suggesting periplasmic Ln are enough to facilitate *pedH* expression[48].

The phenotypes for the *lutH* outer membrane transporter mutant were distinct from the ABC transporter mutant phenotypes. Surprisingly, an approximate 0.6 µM decrease in La^{3+} content from the *lutH* mutant strain culture supernatants was observed. However, since methanol growth did not occur in the *lutH* strain when *mxaF* was also deleted from the genome (Fig. 4c), this suggests that significant quantities of La^{3+} do not enter the cell to trigger *xox1* expression. Lack of La^{3+} transport into the periplasm would explain why the *lutH* mutant was able to grow when *mxaF* was not deleted from the cell; the cell would not sense periplasmic La^{3+} and the *mxa* operon would be expressed. The decrease of La^{3+} from the media likely reflects adsorption of La^{3+} onto the surface of the cells or interaction of La^{3+} with lipopolysaccharide, a phenomenon observed for other metals in different bacterial species[49].

A discovery from this work is that the Ln transport system can be bypassed by suppression or acclimation. Acclimation of the *mxaF lutH* double mutant strain allowed *xoxF1* expression and rapid growth. It may be that Ln can leak into the periplasm slowly over time and once a threshold is reached, *xoxF1* is expressed. A second possibility is that an alternative outer membrane transport system is expressed in the acclimated cultures.

The requirement for the Ln-ABC transport system was bypassed by suppression which allowed growth at reduced rate. Suppressor mutations may facilitate Ln uptake through an alternative system, either by increased expression of such system or by amino acid changes in a different metal import system to facilitate Ln transport. In *Pseudomona putida* KT2440, growth in the absence of the analogous Ln-ABC transporter still occurs if exogenous Ln^{3+} concentrations are high (100 µM) and/or $Fe^{2+/3+}$ concentrations are low. These results suggest that in *P. putida* KT2440, Ln are in competition with metals such as Fe^{3+} and can be transported by other metal (Fe^{3+}) transport systems when in excess[48]. Intriguingly, Gu and Semrau saw differential expression of multiple genes encoding ABC-type and TonB-dependent transporters in the methanotroph, *Methylosinus trichosporium* OB3b, when cerium was added to the growth medium[50]. However, in *M. extorquens* AM1, Good et al. did not observe a similar upregulation of metal transport systems with the addition of La^{3+}[25].

We did not identify transposon insertions in the *lanM* or *lutD* genes though the proteins they encode have been shown to bind Ln[4,33]. These findings are consistent with studies in strain PA1 and suggest a non-essential or redundant role for these gene products[31].

Notably, our transposon mutagenesis study did not identify obvious gene candidates for lanthanophore biosynthesis though over 600 insertions were mapped to the genome. This may indicate that more than one lanthanophore is produced or that the lanthanophore has an essential role that is not yet understood.

Our genetic study identified processes and gene products previously known or predicted to be required for XoxF function such as PQQ and cytochrome synthesis, heme export, and the XoxF, XoxJ, and XoxG proteins themselves. Recent biochemical and structural analyses of XoxG suggest that this cytochrome is tuned specifically for light Ln (lanthanum to samarium), while XoxJ interacts with and may activate XoxF1[22]. Here we show that loss of either *xoxG* or *xoxJ* results in growth that mirrors the *xoxF1 xoxF2* double mutant strain, consistent with XoxG and XoxJ as essential for the activity of XoxF-enzymes. However, using growth and transcriptional reporter fusion studies, we show that unlike XoxF1, XoxG and XoxJ are not required for expression of the *mxa* genes yet loss of the *xoxG* and *xoxJ* genes impacts growth in the absence of La^{3+}. In the methanotroph *Methylomonas* sp. strain LW13, loss of *xoxG* also results in a growth defect in methanol medium lacking Ln suggesting an unknown role in metabolism in addition to functioning as a cytochrome for XoxF-mediated methanol oxidation[36]. Our results are in contrast to previous reports for *M. extorquens* PA1 and AM1, where loss of *xoxG* and *xoxJ* did not result in a growth phenotype in methanol medium lacking Ln[31,51]. Notably, the previous AM1 studies were carried out on agar plates where subtle growth defects may not be apparent.

Strains lacking novel genes were also identified that only displayed a requirement if La^{3+} was provided and include an *mxaD* homolog, *orf6* and *orf7*. MxaD is a 17-kDa periplasmic protein that directly or indirectly stimulates the interaction between the MxaFI-MeDH and cytochrome c_L [52] . Before the existence of Ln-dependent MeDHs was known, it was concluded that *orf6* and *orf7* gene products did not have a role in C_1-metabolism though *orf6* and *orf7* are proximal to other methylotrophy genes[51]. Results here suggest that *orf6* and *orf7* contribute to Ln-dependent methylotrophy.

Our genetic study identified novel gene products that facilitate methanol growth regardless of La^{3+} presence or absence. An ABC-type transporter of unknown function was identified as essential. Lack of a periplasmic binding component suggests an export function rather than import. One possible function for META1p2359 could be the export of PQQ into the periplasm for incorporation into XoxF1 and MxaFI. This hypothesis is consistent with structural analysis of this exporter and the essential role for META1p2359 in methanol oxidation. An aminopeptidase was also identified which may be involved in processing one or more proteins required for XoxF1 and MxaFI function. Alternatively, the aminopeptidase could function in processing PQQ, as PQQ is peptide based and not all PQQ processing proteins have been identified[53,54].

Lastly, our TEM and EDS analyses demonstrate that *M. extorquens* AM1 stores Ln in the cytoplasm in crystal form. For many bacteria, biomineralization is a mechanism used to cope with toxicity of different metals, manage waste products, sense and change orientations in accordance with geomagnetic fields, and store important cations for growth[55–61]. It has been reported that some bacteria store cations like Mg^{2+} and Ca^{2+} complexed to polyphosphate in the form of volutin (also known as metachromatic granules) or acidocalcisomes[62–65]. It is not yet known if *M. extorquens* AM1 stores La^{3+} complexed to polyphosphate, however, the ratios of P, O, and La^{3+} detected in our studies are consistent with La^{3+} phosphates. A gene encoding a putative homospermidine synthase (*hss*) was identified. Homospermidine synthases function in polyamine biosynthesis[66,67]. Polyamines have diverse roles but have been suggested to complex with polyphosphate to reduce spermidine toxicity in *P. aeruginosa* and stabilize polyphosphate granule formation in *Escherichia coli*[68,69]. Detailed studies are necessary to define the exact chemical structure of Ln storage deposits in *M. extorquens* AM1 and if these granules are membrane or lipid bound. Our current findings bring exciting implications for Ln metabolism and for the development of bioremediation and biometallurgy strategies for Ln recovery.

Methods

Bacterial strains and cultivation.

Strains and plasmids used in this study are listed in Table S2. *E. coli* strains were cultivated in Lysogeny Broth (LB) medium[70] (BD, Franklin Lakes, NJ) at 37 °C. *M. extorquens* AM1 strains were grown in *Methylobacterium* PIPES [piperazine-*N,N*'-bis(2-ethanesulfonic acid)] (MP) media[71] supplemented with succinate (15 mM) and/or methanol (125 mM) as described[18] unless otherwise stated. Conjugations took place on Difco Nutrient Agar (Thermo Fisher Scientific, Waltham, MA). Liquid cultures were grown at 29 °C and shaken at 200 and 180 rpm in New Brunswick Innova 2,300 and Excella E25 shaking incubators

(Eppendorf, Hauppauge, NY), respectively. $LaCl_3$ was supplemented to a final concentration of 2 or 20 μM when indicated. When necessary, antibiotics were added at the following concentrations: rifamycin (Rif, 50 μg/mL), tetracycline (Tc, 10 μg/mL for LB, 5 μg/mL for MP or 10 μg/mL when used together with Rif), kanamycin (Km, 50 μg/mL), ampicillin (Ap, 50 μg/mL).

Plasmid and strain construction. Primers used for plasmid and strain construction are listed in Table S3. The allelic exchange plasmid pHV2 was constructed by cloning the *sacB* gene from pCM433[72] into the PscI site of pCM18[73] in the same orientation as the Tc resistance gene. Insertion and orientation of *sacB* was confirmed by colony PCR. The *lutH* transcriptional reporter fusion was constructed by cloning the promoter region of *lutH* into the AclI and EcoRI sites upstream of a promoter-less *venus* gene in pAP5[24]. To create overexpression constructs for complementation studies, individual genes in the *lut* operon (*lutA*, *lutB*, *lutE*, *lutF*, and *lutG)* were cloned into the KpnI and SacI sites downstream of a P_{lac} promoter in pCM62[39]. Diagnostic PCR was used to confirm successful integration of inserts. Plasmids were maintained in *E. coli* TOP10 (Invitrogen, Carlsbad, CA). Gene deletions were constructed using pCM184 or pHV2 as previously described[18] except 5% sucrose was added for counter selection against single crossovers[72] when using pHV2. Plasmids were conjugated into *M. extorquens* AM1 via biparental mating using *E. coli* S17-1[74] or triparental mating using *E. coli* TOP10 (Invitrogen, Carlsbad, CA) and *E. coli* harboring the conjugative plasmid pRK2013 as described[18]. When indicated, the Km resistance cassette was resolved using pCM157 to achieve marker-less deletions[73].

Transposon mutagenesis. Suicide vector pCM639 carrying a mini transposon IS*phoA*/hah-T[75] was conjugated into the *mxaF fae* strain background via triparental mating as described[18,76]. Dilutions of the mating mixtures were plated onto MP succinate (15 mM) plus methanol (50 mM) La^{3+} medium containing 10 μg/mL Tc to select for successful integration of the mini transposon into the *M. extorquens* AM1 genome and 50 μg/mL Rif to counter select against *E. coli* strains bearing pCM639 or pRK2013. Plates were incubated for 5–7 days at 29 °C. Transposon mutant colonies were streaked onto MP succinate methanol La^{3+} Tc medium for downstream studies.

Location of transposon insertions. To identify the transposon insertion sites, genomic DNA was isolated using a Qiagen DNeasy UltraClean Microbial Kit (Qiagen, Germantown, MD). Degenerate nested PCR was performed as described[76,77] with the following exceptions: PCR reactions contained 1 μM of each primer, 0.05 U/μL Dream Taq (Thermo Fisher Scientific, Waltham, MA), and 5% dimethyl sulfoxide. Modifications to the PCR amplification parameters included 2 min for the initial denaturation at 95 °C, 6 cycles of annealing at 40 °C followed by 25 cycles of annealing at 65 °C for the first PCR reaction, and 30 cycles of annealing at 65 °C for the second PCR reaction. PCR products were purified using a Qiagen QIAquick 96 PCR Purification Kit (Germantown, MD). Sequence analysis was performed using TransMapper, a Python-based program developed in-house to identify transposon insertion locations and map them to the *M. extorquens* AM1 genome for visualization using SnapGene Viewer (GSL Biotech LLC, Chicago, IL).

Phenotypic analyses. Growth phenotypes were determined on solid or in liquid MP media using a minimum of three biological replicates. On solid media, colony size was scored after four days. Growth curve experiments were conducted at 29 °C in an Excella E25 shaking incubator (New Brunswick Scientific, Edison, NJ) using a custom-built angled tube rack holder as previously described[18]. Optical density (OD_{600}) was measured at 600 nm using a Spectronic 20D spectrophotometer (Milton Roy Company, Warminster, PA). For strains with extended growth lags, suppression and acclimation was assessed. Strains from the growth curves were streaked onto methanol La^{3+} medium after they reached stationary phase. If the parent stock strain did not grow on methanol La^{3+} medium and the strain post-growth curve grew, acclimation versus suppression was tested. Strains were passaged from the methanol medium plate to a succinate medium plate. After colonies grew on succinate medium, they were streaked back onto methanol La^{3+} medium. If strains retained the ability to grow on methanol medium, it was concluded that growth was due to a suppressor mutation. If strains lost the ability to grow on methanol medium after succinate passage, it was concluded growth was due to acclimation and not a genetic change.

Transcriptional reporter fusion assays. *M. extorquens* AM1 strains carrying *mxa*, *xox1*, and *lutH* transcriptional reporter fusions (Table S2) which use *venus*[78] as a fluorescent reporter were grown in MP media supplemented with methanol only or methanol and succinate with and without La^{3+} as indicated in the text. Once cells reached an OD_{600} of 0.6, expression was measured as relative fluorescent units (RFU) using a SpectraMax M2 plate reader (Molecular Devices, Sunnyvale, CA) and normalized to OD_{600} as previously described[18]. For measurements of *xox1* and *mxa* expression before and after acclimation in the *mxaF lutH* strain, measurements were taken every three hours before after sub-culturing until stationary phase. Expression after acclimation is reported in Table 4 from cells harvested at an OD_{600} of 0.6.

La^{3+} depletion during *M. extorquens* AM1 growth. Overnight cultures of wild type, *lutA*, *lutE*, *lutF*, and *lutH* mutant strains were inoculated 1:50 into 250 mL polycarbonate flasks (Corning Inc., Corning, NY) containing 75 mL of MP medium [71]. Succinate (3.75 mM) and methanol (125 mM) were added as carbon sources with 2 μM $LaCl_3$. Flasks were incubated at 28 °C at 200 rpm in Innova 2,300 shaking incubators (Eppendorf, Hauppauge, NY) for 44 h. To monitor La^{3+} depletion during *M. extorquens* AM1 cultivation, the Arsenazo III assay was used[79]. 5 mL samples were collected at four different time points (2, 12, 16, and 24 h) and the concentration of La^{3+} remaining in the supernatant was calculated using the calibration curve prepared as previously described[79]. A control of three uninoculated flasks containing MP medium with 2 µM $LaCl_3$ were considered to determine La^{3+} adsorption by the flasks which was subtracted from the culture measurements. The initial concentration of La^{3+} in the media (before growth) was measured using the Arsenazo III assay in the same way as described above. Significant differences between depletion of La^{3+} by different strains were calculated using One-way ANOVA followed by a t-test.

Cellular locations of Ln visualized using transmission electron microscopy (TEM). Sample preparation for TEM: wild type, *lutA*, *lutE*, *lutF*, and *lutH* mutant strains were grown in MP medium containing 125 mM methanol and 3.75 mM succinate as carbon sources with or without the addition of 20 µM $LaCl_3$ until they reached an OD_{600} of ~ 0.6. 3 mL of cells was harvested by centrifugation for 3 min at 1,500×*g* at room temperature and fixed for 30 min in 1 mL of 2.5% (v/v) glutaraldehyde (Electron Microscopy Sciences, Hatfield, PA) in 0.1 M cacodylate buffer (Electron Microscopy Sciences, Hatfield, PA). After fixation, cells were pelleted by centrifugation for 3 min at 1,500×*g* and washed with 1 mL of 0.1 M cacodylate buffer. Cell pellets were embedded in 2% (w/v) agarose and washed three times with 0.1 M cacodylate buffer. When indicated, pellets in agarose blocks were stained for 30 min in 1% osmium tetroxide in 0.1 M cacodylate buffer. Samples were washed three times with 0.1 M cacodylate buffer, dehydrated in acetone, and embedded in Spurr resin (Electron Microscopy Sciences, Hatfield, PA). Blocks were polymerized at 60ºC for 48 h. 70 nm sections were obtained with a Power Tome XL ultramicrotome (RMC Boeckeler Instruments, Tucson AZ), deposited on 200 mesh carbon coated grids, and stained with 2% uranyl acetate (Electron Microscopy Sciences, Hatfield, PA). To assess the presence of La^{3+} by EDS, sections were left unstained. To image the distribution of cellular La^{3+}, a TEM JOEL 1,400 Flash (Japan Electron Optics Laboratory, Tokyo, Japan) was used. Detection of La^{3+} in the cells and high-resolution imaging were done with a JEOL 2200FS (Japan Electron Optics Laboratory, Tokyo, Japan) operated at 200 kV. X-ray energy dispersive spectroscopy was performed using an Oxford Instruments INCA system (Abingdon, United Kingdom).

Received: 4 March 2020; Accepted: 9 July 2020
Published online: 29 July 2020

References

1. Zepf, V., Reller, A., Rennie, C., Ashfield, M. & Simmons, J. *Materials Critical to the Energy Industry. An Introduction.* (BP, 2014).
2. Martinez-Gomez, N. C., Vu, H. N. & Skovran, E. Lanthanide chemistry: from coordination in chemical complexes shaping our technology to coordination in enzymes shaping bacterial metabolism. *Inorg. Chem.* **55**, 10083–10089 (2016).
3. Teo, R. D., Termini, J. & Gray, H. B. Lanthanides: applications in cancer diagnosis and therapy. *J. Med. Chem.* **59**, 6012–6024 (2016).
4. Mattocks, J. A., Ho, J. V. & Cotruvo, J. A. A selective, protein-based fluorescent sensor with picomolar affinity for rare earth elements. *J. Am. Chem. Soc.* **141**, 2857–2861 (2019).
5. Hibi, Y. *et al.* Molecular structure of La3+-induced methanol dehydrogenase-like protein in *Methylobacterium radiotolerans*. *J. Biosci. Bioeng.* **111**, 547–549 (2011).
6. Pol, A. *et al.* Rare earth metals are essential for methanotrophic life in volcanic mudpots. *Environ. Microbiol.* **16**, 255–264 (2014).
7. Nakagawa, T. *et al.* A catalytic role of XoxF1 as La3+-dependent methanol dehydrogenase in *Methylobacterium extorquens* strain AM1. *PLoS ONE* **7**, e50480 (2012).
8. Fitriyanto, N. A. *et al.* Ce 3+ -induced exopolysaccharide production by *Bradyrhizobium* sp. MAFF211645. *J. Biosci. Bioeng.* **111**, 146–152 (2011).
9. Wehrmann, M., Billard, P., Martin-Meriadec, A., Zegeye, A. & Klebensberger, J. Functional role of lanthanides in enzymatic activity and transcriptional regulation of pyrroloquinoline quinone-dependent alcohol dehydrogenases in *Pseudomonas putida* KT2440. *MBio* **8**, e00570-e617 (2017).
10. Wehrmann, M., Berthelot, C., Billard, P. & Klebensberger, J. The PedS2/PedR2 two-component system is crucial for the rare earth element switch in *Pseudomonas putida* KT2440. *mSphere* **3**, e00376–e003718 (2018).
11. Wang, L. *et al.* Lanthanide-dependent methanol dehydrogenase from the legume symbiotic nitrogen-fixing bacterium *Bradyrhizobium diazoefficiens* strain USDA110. *Enzyme Microb. Technol.* **130**, 109371 (2019).
12. Skovran, E. & Martinez-Gomez, N. C. Just add lanthanides. *Science* **348**, 862–863 (2015).
13. van Teeseling, M. C. F. *et al.* Expanding the verrucomicrobial methanotrophic world: description of three Novel Species of Methylacidimicrobium gen nov. *Appl. Environ. Microbiol.* **80**, 6782–6791 (2014).
14. Huang, J. *et al.* Rare earth element alcohol dehydrogenases widely occur among globally distributed, numerically abundant and environmentally important microbes. *ISME J.* **13**, 2005–2017 (2019).
15. Keltjens, J. T., Pol, A., Reimann, J. & Op Den Camp, H. J. M. PQQ-dependent methanol dehydrogenases: rare-earth elements make a difference. *Appl. Microbiol. Biotechnol.* **98**, 6163–6183 (2014).
16. Chistoserdova, L. Lanthanides: new life metals?. *World J. Microbiol. Biotechnol.* **32**, 138 (2016).
17. Good, N. M. *et al.* Pyrroloquinoline quinone-containing ethanol dehydrogenase in *Methylobacterium extorquens* AM1 extends lanthanide-dependent metabolism to multi-carbon substrates. *J. Bacteriol.* **198**, 3109–3118 (2016).
18. Vu, H. N. *et al.* Lanthanide-dependent regulation of methanol oxidation systems in *Methylobacterium extorquens* AM1 and their contribution to methanol growth. *J. Bacteriol.* **198**, 1250–1259 (2016).
19. Prejanò, M., Iziana Marino, T., Russo, N., Marino, T. & Russo, N. How can methanol dehydrogenase from *Methylacidiphilum fumariolicum* work with the alien Ce III ion in the active center? A theoretical study. *Chem. A Eur. J.* **23**, 8652–8657 (2017).
20. McSkimming, A., Cheisson, T., Carroll, P. J. & Schelter, E. J. functional synthetic model for the lanthanide-dependent quinoid alcohol dehydrogenase active site. *J. Am. Chem. Soc.* **140**, 1223–1226 (2018).
21. Lumpe, H., Pol, A., Op Den Camp, H. & Daumann, L. Impact of the lanthanide contraction on the activity of a lanthanide-dependent methanol dehydrogenase: a kinetic and DFT study and DFT study. *Dalt. Trans.* **47**, 10463–10472 (2018).
22. Featherston, E. R. *et al.* Biochemical and structural characterization of XoxG and XoxJ and their roles in lanthanide-dependent methanol dehydrogenase activity. *ChemBioChem* **20**, 2360–2372 (2019).
23. Chistoserdova, L., Chen, S.-W., Lapidus, A. & Lidstrom, M. E. Methylotrophy in *Methylobacterium extorquens* AM1 from a genomic point of view. *J. Bacteriol.* **185**, 2980–2987 (2003).

24. Skovran, E., Palmer, A. D., Rountree, A. M., Good, N. M. & Lidstrom, M. E. XoxF is required for expression of methanol dehydrogenase in *Methylobacterium extorquens* AM1. *J. Bacteriol.* **193**, 6032–6038 (2011).
25. Good, N. M., Moore, R. S., Suriano, C. J. & Martinez-Gomez, N. C. Contrasting in vitro and in vivo methanol oxidation activities of lanthanide-dependent alcohol dehydrogenases XoxF1 and ExaF from *Methylobacterium extorquens* AM1. *Sci. Rep.* **9**, 4248 (2019).
26. Chu, F., Beck, D. A. C. & Lidstrom, M. E. MxaY regulates the lanthanide-mediated methanol dehydrogenase switch in *Methylomicrobium buryatense*. *PeerJ* **4**, e2435 (2016).
27. Semrau, J. Uptake and effect of rare earth elements on gene expression in *Methylosinus trichosporium*. *OB_3b* **363**, fnw129 (2016).
28. Masuda, S. *et al.* Lanthanide-dependent regulation of methylotrophy in *Methylobacterium aquaticum* Strain 22A. *mSphere* **3**, e00462-17 (2018).
29. Skovran, E., Raghuraman, C. & Martinez-Gomez, N. C. Lanthanides in methylotrophy. *Methyl. Methyl. Communit.* **1**, 101–116 (2019).
30. Springer, A. L., Morris, C. J. & Lidstrom, M. E. Molecular analysis of mxbD and mxbM, a putative sensor-regulator pair required for oxidation of methanol in *Methylobacterium extorquens* AM1. *Microbiology* **143**, 1737–1744 (1997).
31. Ochsner, A. M. *et al.* Use of rare-earth elements in the phyllosphere colonizer *Methylobacterium extorquens* PA1. *Mol. Microbiol.* **111**, 1152–1166 (2019).
32. Daumann, L. J. Essential and ubiquitous: the emergence of lanthanide metallobiochemistry. *Angew. Chem. Int. Ed.* **58**, 12795–12802 (2019).
33. Cotruvo, Jr., J. A., Featherston, E. R., Mattocks, J. A., Ho, J. V. & Laremore, T. N. Lanmodulin: a highly selective lanthanide-binding protein from a lanthanide-utilizing bacterium. *J. Am. Chem. Soc.* **140**, 15056–15061 (2018).
34. Sawyer, E. B. & Barker, P. D. Continued surprises in the cytochrome c biogenesis story. *Protein Cell* **3**, 405–409 (2012).
35. Versantvoort, W. *et al.* Characterization of a novel cytochrome c as the electron acceptor of XoxF-MDH in the thermoacidophilic methanotroph *Methylacidiphilum fumariolicum* SolV. *Biochim. Biophys. Acta* **1867**, 595–603 (2019).
36. Zheng, C., Huang, Y., Zhao, J. & Chistoserdova, F. Physiological effect of XoxG(4) on lanthanide-dependent methanotrophy. *MBio* **9**, e02430-e2517 (2018).
37. Söding, J., Biegert, A. & Lupas, A. N. The HHpred interactive server for protein homology detection and structure prediction. *Nucleic Acids Res.* **33**, W244–W248 (2005).
38. Baek, M., Park, T., Heo, L., Park, C. & Seok, C. GalaxyHomomer: a web server for protein homo-oligomer structure prediction from a monomer sequence or structure. *Nucleic Acids Res.* **45**, W320–W324 (2017).
39. Chou, H.-H. & Marx, C. J. Optimization of gene expression through divergent mutational paths. *Cell Rep.* **1**, 133–140 (2012).
40. Klaus, T., Joerger, R., Olsson, E. & Granqvist, C.-G. Silver-based crystalline nanoparticles, microbially fabricated. *Proc. Natl. Acad. Sci.* **96**, 13611–13614 (1999).
41. Groom, J. D., Ford, S. M., Pesesky, M. W. & Lidstrom, M. E. A mutagenic screen identifies a TonB-dependent receptor required for the lanthanide metal switch in the type I methanotroph *Methylotuvimicrobium buryatense* 5GB1C. *J. Bacteriol.* **201**, e00120-19 (2019).
42. Maleke, M. *et al.* Biomineralization and bioaccumulation of europium by a thermophilic metal resistant bacterium. *Front. Microbiol.* **10**, 1–10 (2019).
43. Leeson, T. S. & Higgs, G. Lanthanum as an intracellular stain for electron microscopy. *Histochem. J.* **14**, 553–560 (1982).
44. Bayer, M. E. & Bayer, M. H. Lanthanide accumulation in the periplasmic space of *Escherichia coli* B. *J. Bacteriol.* **173**, 141–149 (1991).
45. Merroun, M. L., Ben Chekroun, K., Arias, J. M. & Alez-Munoz, M. T. G. A. Lanthanum fixation by *Myxococcus xanthus:* cellular location and extracellular polysaccharide observation. *Chemosphere* **52**, 113–120 (2003).
46. Hashimoto, H. & Mannami, M. N. T. Dynamical theory of electron diffraction for the electron microscopic image of crystal lattices. II. Image of superposed crystals (Moiré pattern). *Philos. Trans. R. Soc.* **253**, 490–516 (1961).
47. Good, N. M. *et al.* Lanthanide-dependent alcohol dehydrogenases require an essential aspartate residue for metal coordination and enzymatic function. *J. Biol. Chem.* **295**, 8272–8284 (2020)
48. Wehrmann, M., Berthelot, C., Billard, P. & Klebensberger, J. Rare earth element (REE)-dependent growth of *Pseudomonas putida* KT2440 relies on the ABC-transporter Peda1A2BC and is influenced by iron availability. *Front. Microbiol.* **10**, 2494 (2019).
49. Langley, S. & Beveridge, T. J. Effect of O-side-chain-lipopolysaccharide chemistry on metal binding. *Appl. Environ. Microbiol.* **65**, 489–498 (1999).
50. Gu, W. & Semrau, J. D. Copper and cerium-regulated gene expression in *Methylosinus trichosporium* OB3b. *Appl Microbiol Biotechnol.* **101**, 8499–8516 (2017).
51. Chistoserdova, L. & Lidstrom, M. E. Molecular and mutational analysis of a DNA region separating two methylotrophy gene clusters in *Methylobacterium extorquens* AM1. *Microbiology* **143**, 1729–1736 (1997).
52. Toyama, H., Inagaki, H., Matsushita, K., Anthony, C. & Adachi, O. The role of the MxaD protein in the respiratory chain of *Methylobacterium extorquens* during growth on Methanol. *Biochim. Biophys. Acta* **1647**, 372–375 (2003).
53. Martins, A. M. *et al.* A two-component protease in *Methylorubrum extorquens* with high activity toward the peptide precursor of the redox cofactor pyrroloquinoline quinone. *J. Biol. Chem.* **294**, 15025–15036 (2019).
54. Bultreys, A. & Gheysen, I. Production and comparison of peptide siderophores from strains of distantly related Pathovars of *Pseudomonas syringae* and *Pseudomonas viridiflava* LMG 2352. *Appl. Environ. Microbiol.* **66**, 325–331 (2000).
55. Zhan, G., Li, D. & Zhang, L. Aerobic bioreduction of nickel(II) to elemental nickel with concomitant biomineralization. *Appl. Microbiol. Biotechnol.* **96**, 273–281 (2012).
56. Bai, H. J., Zhang, Z. M., Guo, Y. & Yang, G. E. Biosynthesis of cadmium sulfide nanoparticles by photosynthetic bacteria *Rhodopseudomonas palustris*. *Colloids Surf. B* **70**, 142–146 (2009).
57. Sousa, T., Chung, A.-P., Pereira, A., Piedade, A. P. & Morais, P. V. Aerobic uranium immobilization by *Rhodanobacter* A2–61 through formation of intracellular uranium-phosphate complexes. *Metallomics* **5**, 390–397 (2013).
58. Couradeau, E. *et al.* An early-branching microbialite cyanobacterium forms intracellular carbonates. *Science* **336**, 459–462 (2012).
59. Debieux, C. M. *et al.* A bacterial process for selenium nanosphere assembly. *Proc. Natl. Acad. Sci.* **108**, 13480–13485 (2011).
60. Rahn-Lee, L. & Komeili, A. The magnetosome model: Insights into the mechanisms of bacterial biomineralization. *Front. Microbiol.* **4**, 352 (2013).
61. Chandrangsu, P., Rensing, C. & Helmann, J. D. Metal homeostasis and resistance in bacteria. *Nat. Rev. Microbiol.* **15**, 338–350 (2017).
62. Kulaev, I. *The Biochemistry of Inorganic Polyphosphates* (Wiley, Hoboken, 1979).
63. Friedberg, I. & Avigad, G. Structures containing polyphosphate in *Micrococcus lysodeikticus*. *J. Bacteriol.* **96**, 544–553 (1968).
64. Pallerla, S. R. *et al.* Formation of volutin granules in *Corynebacterium glutamicum*. *FEMS Microbiol. Lett.* **243**, 133–140 (2005).
65. Widra, A. Metachromatic granules of microorganisms. *J. Bacteriol.* **78**, 664–670 (1959).
66. Krossa, S., Faust, A., Ober, D. & Scheidig, A. J. Comprehensive structural characterization of the bacterial homospermidine synthase-an essential enzyme of the polyamine metabolism. *Sci. Rep.* **6**, 19501 (2015).
67. Wortham, B. W., Patel, C. N. & Oliveira, M. Polyamines in bacteria: pleiotropic effects yet specific mechanisms. *Adv. Exp. Med. Biol.* **603**, 106–115 (2007).

68. Peng, Y. C., Lu, C. Y., Li, G., Eichenbaum, Z. & Lu, C. D. Induction of the pho regulon and polyphosphate synthesis against spermine stress in *Pseudomonas aeruginosa*. *Mol. Microbiol.* **104**, 1037–1051 (2017).
69. Motomura, K., Takiguchi, N., Ohtake, H. & Kuroda, A. Polyamines affect polyphosphate accumulation in *Escherichia coli*. *J. Environ. Biotechnol.* **6**, 41–46 (2006).
70. Bertani, G. Studies on lysogenesis. I. The mode of phage liberation by lysogenic *Escherichia coli*. *J. Bacteriol.* **62**, 293–300 (1951).
71. Delaney, N. F. *et al.* Development of an optimized medium, strain and high-throughput culturing methods for *Methylobacterium extorquens*. *PLoS ONE* **8**, e62957 (2013).
72. Marx, C. J. Development of a broad-host-range sacB-based vector for unmarked allelic exchange. *BMC Res. Notes* **1**, 1 (2008).
73. Marx, C. J. & Lidstrom, M. E. Broad-host-range Cre-lox system for antibiotic marker recycling in gram-negative bacteria. *Biotechniques* **33**, 1062–1067 (2002).
74. Simon, R., Priefer, U. & Pühler, A. A broad host range mobilization system for in vivo genetic engineering: transposon mutagenesis in gram negative bacteria. *Nat. Biotechnol.* **1**, 784–791 (1983).
75. Jacobs, M. A. *et al.* Comprehensive transposon mutant library of *Pseudomonas aeruginosa*. *Proc. Natl. Acad. Sci.* **100**, 14339–14344 (2003).
76. Marx, C. J., O'Brien, B. N., Breezee, J. & Lidstrom, M. E. Novel methylotrophy genes of *Methylobacterium extorquens* AM1 identified by using transposon mutagenesis including a putative dihydromethanopterin reductase. *J. Bacteriol.* **185**, 669–673 (2003).
77. Manoil, C. & Traxler, B. Insertion of in-frame sequence tags into proteins using transposons. *Methods* **20**, 55–61 (2000).
78. Nagai, T. *et al.* A variant of yellow fluorescent protein with fast and efficient maturation for cell-biological applications. *Nat. Biotechnol.* **20**, 87–90 (2002).
79. Hogendoorn, C. *et al.* Facile arsenazo III-based assay for monitoring rare earth element depletion from cultivation media for methanotrophic and methylotrophic bacteria. *Appl. Environ. Microbiol.* **84**, e02887-e2917 (2018).

Acknowledgements

We would like to thank Dr. Lena Daumann and Dr. Nathan Good for critical review of this manuscript. We would like to thank SJSU General Microbiology students who isolated transposon mutants and purified genomic DNA for sequencing as part of a class research project. The mutant hunt in this study was inspired by Dr. Elizabeth Skovran's undergraduate research mentor, Dr. Marc Rott at the University of Wisconsin-LaCrosse. We would like to thank Timothy Andriese for assistance with sequencing of the transposon mutant DNA and all Skovran lab members for assistance with growth curves and transcriptional reporter fusion assays. TEM work was done at the Center for Advanced Microscopy, MSU. We would like to thank Dr. Alicia Withrow for invaluable assistance with TEM experiments and Dr. Xudong Fan for his expertise using TEM-EDS. This material is based upon work supported by the National Science Foundation under Grant No. 1750003 and by a California State University Program for Education and Research in Biotechnology (CSUPERB) Joint Venture Grant. P.R-J. was supported by the National Science Foundation under Grant No. 1750003. E.M.A and F.Y. were supported by the National Science Foundation Research Initiative for Scientific Enhancement (RISE) award under Grant No. R25GM071381. F.Y. was also supported by the National Institute of Health Maximizing Access to Research Careers Undergraduate Student Training in Academic Research (MARC U-STAR) award under Grant No. 4T34GM008253. Funding for transposon DNA isolation, PCR, and sequencing was provided by San José State University through the Department of Biological Sciences.

Author contributions

E.S., N.C.M-G., P.R-J., and H.N.V. directed experiments. N.C.M-G., and E.S. wrote the manuscript. P.R-J. conducted microscopy and Ln transport experiments. H.N.V, G.A.S, J.C., and E.C carried out transposon mutagenesis studies. H.N.V., G.A.S., R.C., J.C., C.R., E.M.A., E.C., N.F.L., and F.Y. constructed strains and conducted growth experiments. R.C., C.H., J.P.W., and G.A.S. conducted expression studies. R.T.N created TransMapper.

Competing interests

The authors declare no competing interests.

Additional information

Supplementary information is available for this paper at https://doi.org/10.1038/s41598-020-69401-4.

Correspondence and requests for materials should be addressed to N.C.M.-G. or E.S.